Supplementary Information

Ligands Defect Engineered NH_2-MIL-88B(Fe) for Efficient Oxygen Evolution Reaction in alkaline seawater

Dongling Xie[a], Jianan Wang[a], Bo Huang[a], Yiyi Yang[a], Dunmin Lin[a], Chenggang Xu[a], Fengyu Xie[a,*]

[a]College of Chemistry and Materials Science, Sichuan Normal University, Chengdu 610066, P. R. China

*Corresponding author. E-mail: [*] xiefengyu161@163.com

Experimental

Reagents and materials

All chemical regents were analytically pure. Nickel foam (NF; area: 2 cm × 3 cm) was bought from Shenzhen Yunfei Materials Co., Ltd. Ferric nitrate hydrate ($Fe(NO_3)_3·9H_2O$; Aladdin), Acetic acid (CH_3COOH; Aladdin), 2-aminoteephthalic acid (H_2ATA, Macklin), anhydrous ethanol (EtOH), sodium hydroxide (NaOH; Chengdu Kelong Chemical Reagent Co.), N,N-dimethylformamide (DMF; Chengdu Haijun Chemical Co., Ltd), potassium hydroxide (KOH; Macklin), ruthenium oxide (RuO_2; Aladdin), nafion ($C_{10}H_7OH$; Beijing Chemical). The deionized water was prepared in the laboratory.

Preparation of NH_2-MIL-88B(Fe)

Firstly, 0.7244 g (4 mmol) of $C_8H_7NO_4$ and 2mL NaOH (0.4 M) were added to 35 mL of DMF. The solution was stirred for 15 minutes and added 2.5 mL ethanol and 2.5 mL deionized water successively. Then add ferric nitrate hydrate 0.404 g $Fe(NO_3)_3·9H_2O$(1 mmol) .Next, the mixed solution was stirred for 30 minutes before pouring into a 50 ml autoclave. At last, the reaction kettle was placed in an oven at 125℃ for 12 hours, and then it was naturally cooled down to room temperature. The material was rinsed several times with DMF, ethanol and deionized water sequentially, and then in a vacuum oven at 60 ℃ overnight to dry.

Preparation of NH_2-MIL-88B(Fe)-xH

The synthesis method of NH_2-MIL-88B(Fe)-3H was similar to the above-mentioned process, and x mL(x=1、2、3、5、7 mL) HAC was doped in the homogeneous solution.

Characterizations

Powder X-ray diffraction (PXRD) data were acquired from a LabX XRD-6100 X-ray diffractometer with Cu Kα radiation (40 kV, 30 mA) and a 0.154 nm wavelength (Shimadzu, Osaka, Japan) within the range of 2θ = 5~70°. Fourier transform infrared (FT-IR) was carried out on an FTIR spectrometer (Theromo Nicolet Corporation, Madison, WI, USA) using the potassium bromide pellet method at an ambient temperature. A TGDTA7300 instrument was used for thermogravimetric analysis from 25℃ to 600℃. A heating rate of 5 ℃/min was used in an air atmosphere. Scanning electron microscope (SEM) images were obtained using a XL30 ESEM FEG at a 20 kV accelerating voltage. The transmission electron microscope (TEM) and energy dispersive X-Ray (EDX) data were collected using a FEI Tecnai G2 F20 (FEI Company, Hillsboro, OR, USA) and OXFORD X-max 80T (FEI Company, Hillsboro, OR, USA). A Thermo Scientifific K-Alpha X-ray photoelectron spectrometer (Thermo Fisher Scientifific, Waltham, MA, USA) using Al was used to acquire X-ray photoelectron spectroscopy (XPS) spectra. 1H NMR spectra were measured on Bruker 600 MHz instruments. After pretreating 10 mg of solid at 150 ℃ for 2 hours, 0.5 mL of 1 M NaOH in D_2O was added to the solid and sonicated the digest for 30 min, then let to set overnight. Finally, the digest was centrifuged and transferred to the NMR tube.

Electrochemical Measurements

All electrochemical performance was measured in a three-electrode system using an electrochemical workstation (CHI 660E) in 1.0 M KOH solution and 1 M KOH +0.5 M NaCl at room temperature. The working electrode was NH_2-MIL-88B(Fe) or NH_2-MIL-88B(Fe)-3H, the counter electrode was a graphite plate, and Hg/HgO electrode was used as the reference. For comparison, RuO_2/NF electrode was made by coating the ink (10 mg RuO_2 mixed with 200 μL ethanol, 600 μL of ethylene glycol and 200 μL Nafion solution with adequate ultrasonic treatment) on a piece of NF (0.5×2 cm^2). All electrochemical measurements were performed after 30 cycles of cyclic voltammetry (CV) test. The pH value of the 1.0 M KOH electrolyte is 14. Linear sweep

voltammetry (LSV) was performed at a scan rate of 5 mV s^{-1}. 90% iR compensation was applied for LSV tests.

The potential E_{RHE} and overpotential (η) were calculated using the following equations:

$$E_{RHE}=E_{Hg/HgO}+(0.098+0.059\times PH)\ V$$

$$\eta=E_{RHE}-1.23\ V$$

Electrochemical surface area (ECSA)

Electrochemical surface areas (ECSAs) were evaluated by measuring the double-layer capacitance (C_{dl}) via CV. CV curves were measured at various scan rates from 20 to 100 mV s^{-1} under the potential window from 0.21 to 0.31 V [1]. According to the following equation, the ECSAs of the series catalysts were calculated:

$$\mathrm{ECSA}=\frac{C_{dl}}{C_s}$$

where Cs is the specific capacitance per unit area for samples under identical electrolyte conditions. For our estimates of surface area, we use the general specific capacitances of Cs =0.040 mF·cm^{-2} in 1.0 M KOH as previously reported. The ECSA-normalized current density for as-prepared catalysts was calculated by:

$$\text{ECSA-normalized current density} = \text{current density} / \text{ECSA}$$

Turnover frequency (TOF) test

Turnover frequency (TOF) can be calculated to further estimate the intrinsic activity of catalysts, which follows the equation:

$$\mathrm{TOF}=\frac{J\times A}{4\times F\times \mathrm{m}}$$

where J is the current density (A cm^{-2}) at a given overpotential of 0.30 V, A and m are the area of the electrode (0.25 cm^{-2}) and the number of loading moles of the active substance on the substrate, respectively. The number 4 represents a four-electron transfer process of OER. F is the Faraday constant (96,485 C mol^{-1}) [2].

The alkaline OER process is considered as four proton-transfer steps:

$$4OH^- = O_2 + 2H_2O + 4e^-$$

The specific reaction steps are given as follows:

$$* + OH_- \rightarrow * OH + e^-$$

$$* OH + OH^- \rightarrow * O + H_2O + e^-$$

$$* O + OH^- \rightarrow * OOH + e^-$$

$$* OOH + OH^- \rightarrow * O_2 + H_2O + e^-$$

$$* O_2 \rightarrow * + O_2$$

Electrochemical stability test

The long-term durability of NH_2-MIL-88B(Fe)-3H was assessed by i-t test in 1 M potassium hydroxide and 1 M KOH + 0.5 M NaCl solution. Voltage of was provided to achieve current densities close to further understand the stability of the material at high current densities.

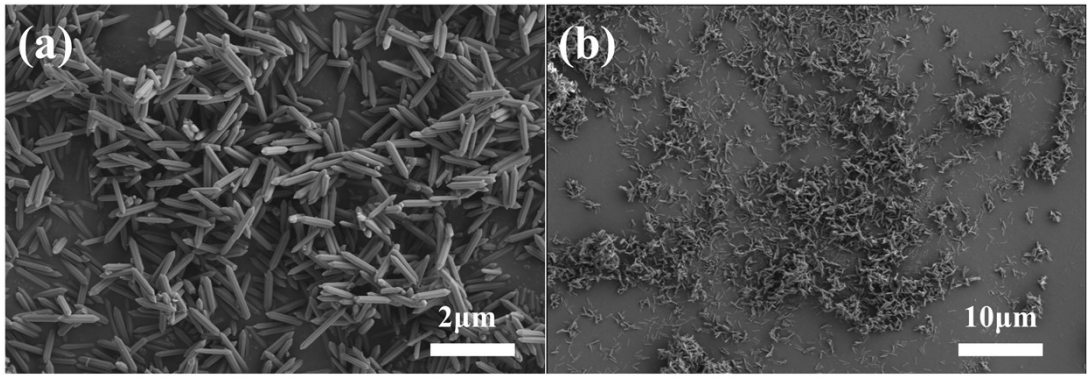

Figure. S1 (a, b) SEM images of NH_2-MIL-88B(Fe)-1H.

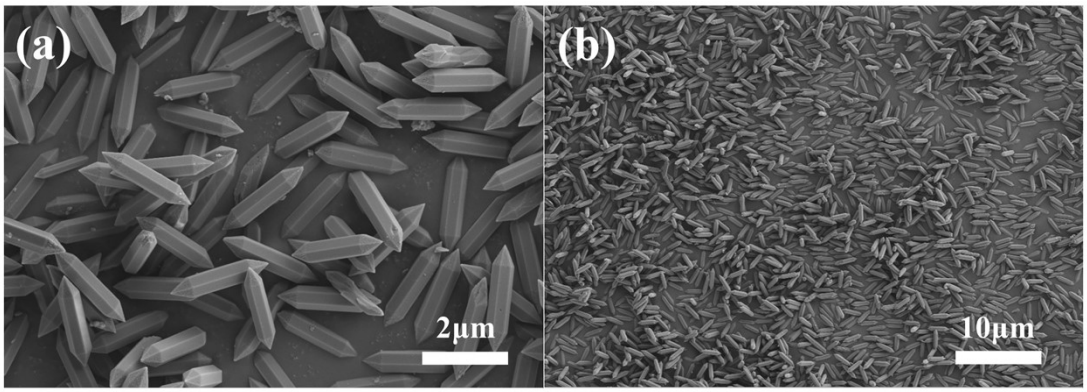

Figure. S2 (a, b) SEM images of NH_2-MIL-88B(Fe)-2H.

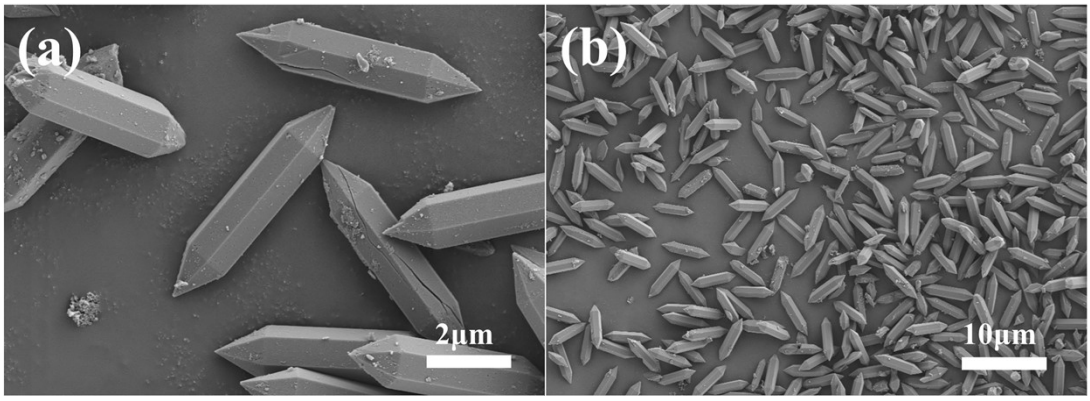

Figure. S3 (a, b) SEM images of NH_2-MIL-88B(Fe)-5H.

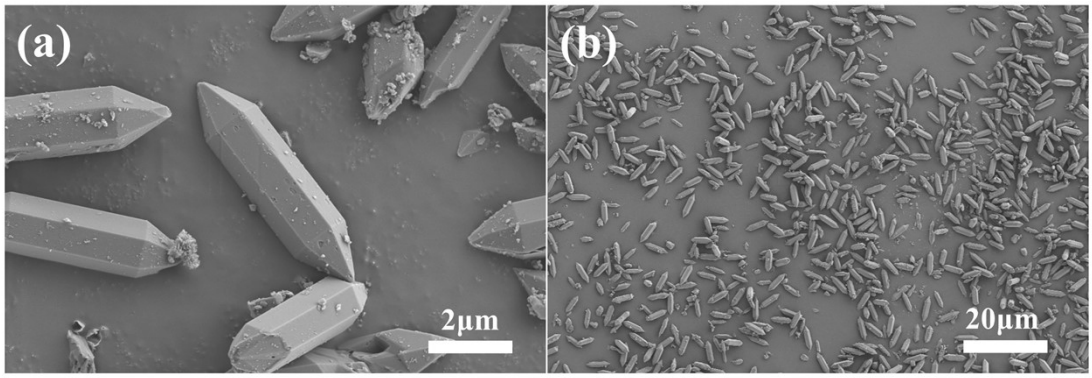

Figure. S4 (a, b) SEM images of NH_2-MIL-88B(Fe)-7H.

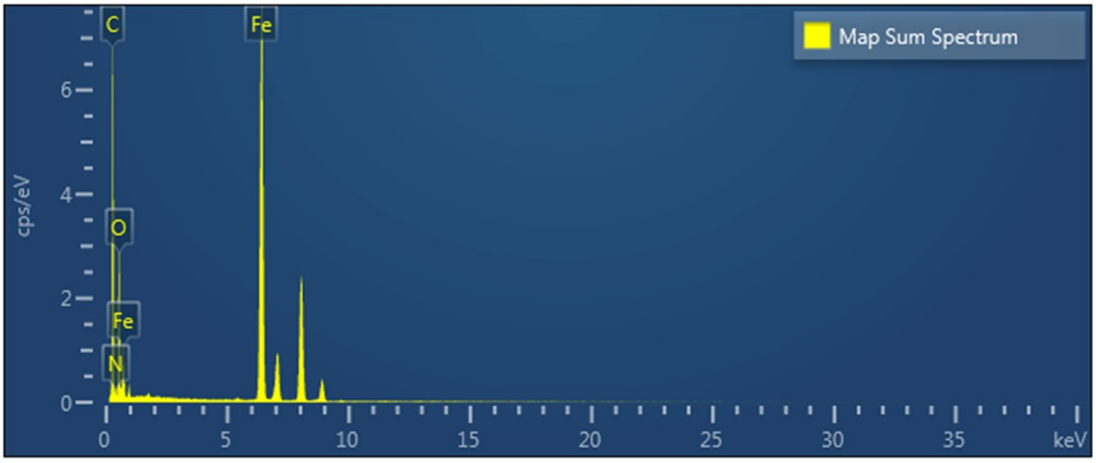

Figure. S5 EDX spectrum of NH_2-MIL-88B(Fe)-3H.

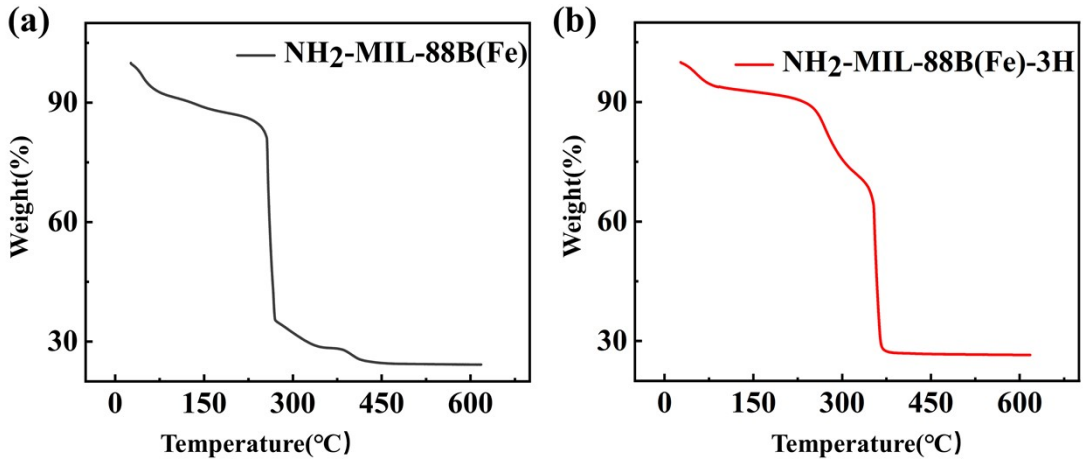

Figure. S6 TGA spectra of (a) NH_2-MIL-88B(Fe) and (b) NH_2-MIL-88B(Fe)-3H.

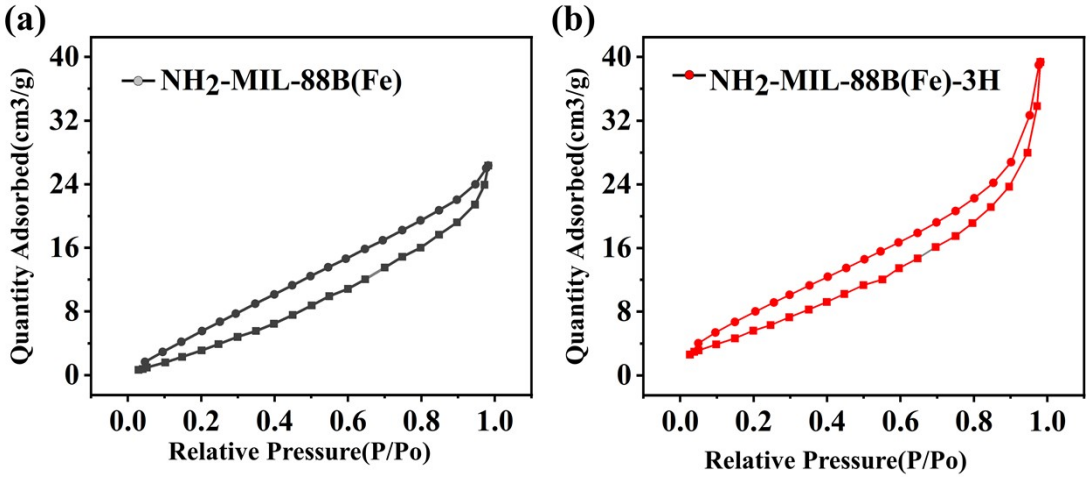

Figure. S7 N_2 sorption isotherms for (a) NH_2-MIL88-B(Fe) and (b)NH_2-MIL-88B(Fe)-3H.

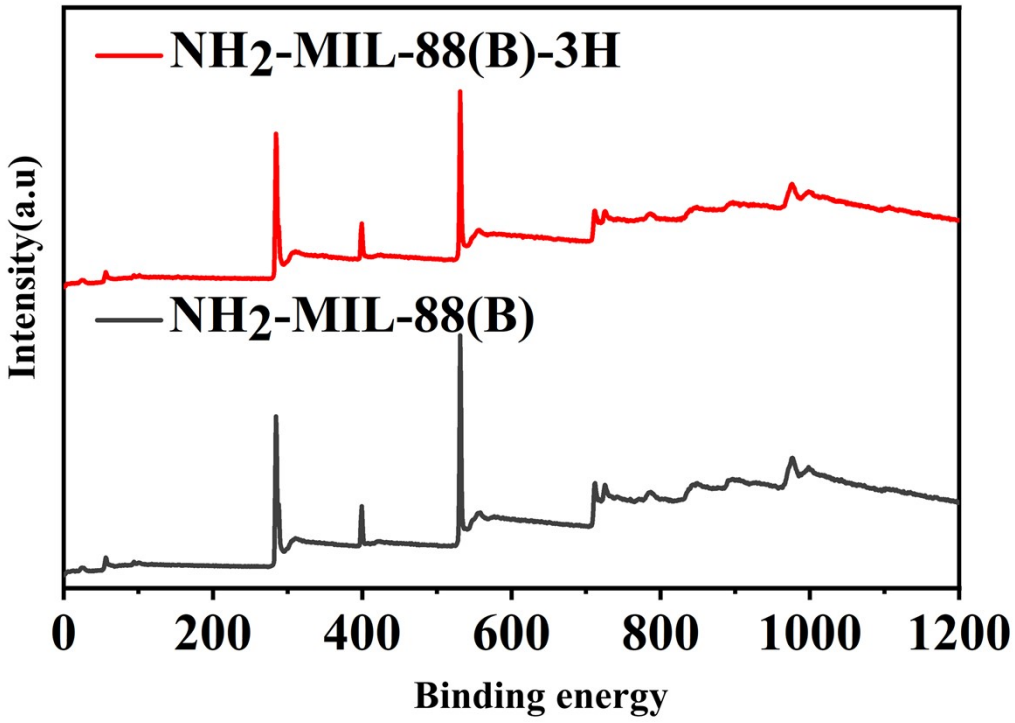

Figure. S8 Full spectrum of NH_2-MIL88-B(Fe) and NH_2-MIL-88B(Fe)-3H.

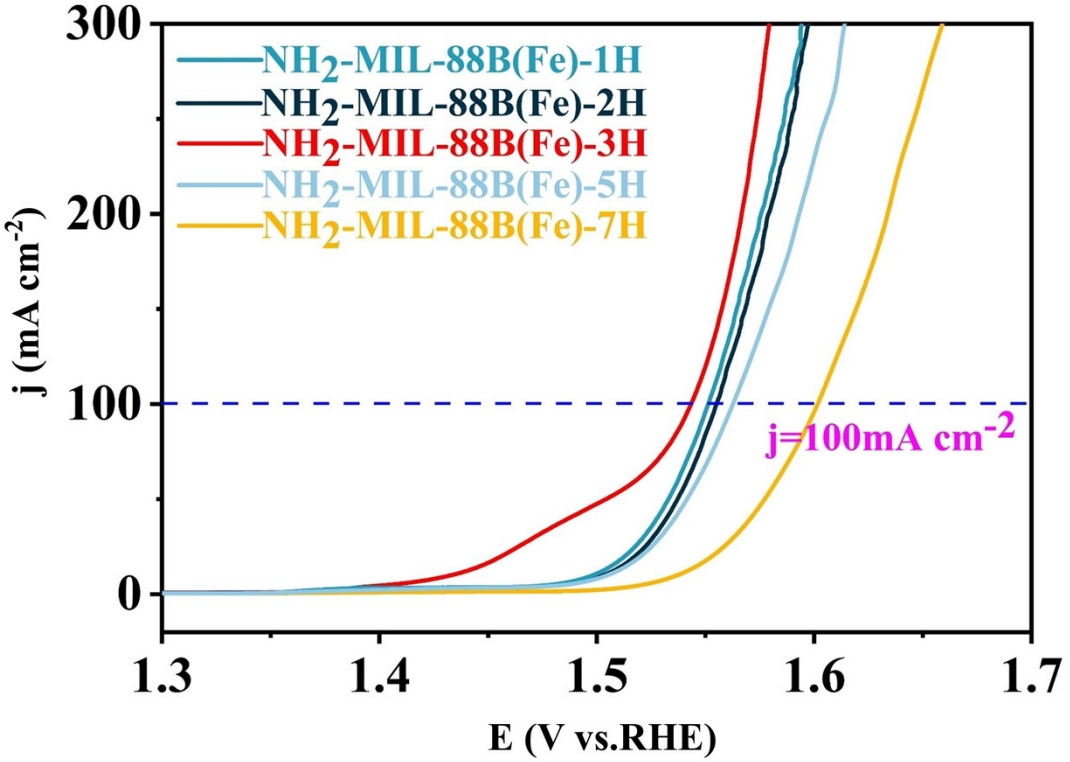

Figure. S9 Comparison of overpotential magnitudes at different current densities in 1M KOH.

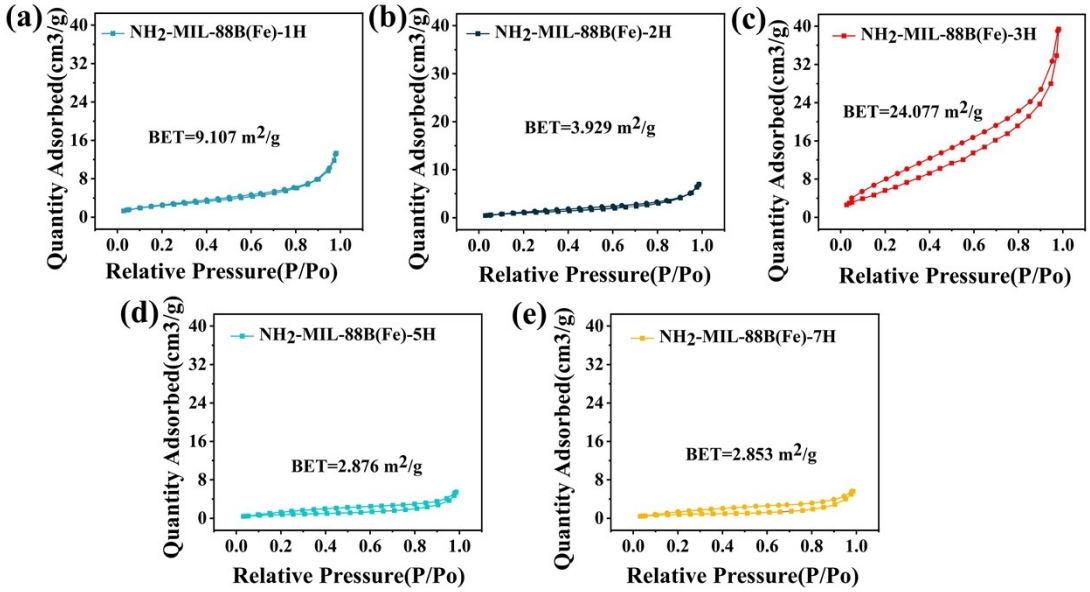

Figure. S10 N_2 sorption isotherms for (a) NH_2-MIL88-B(Fe), (b) NH_2-MIL-88B(Fe)-2H, (c) NH_2-MIL-88B(Fe)-3H, (d) NH_2-MIL-88B(Fe)-5H, (e) NH_2-MIL-88B(Fe)-7H.

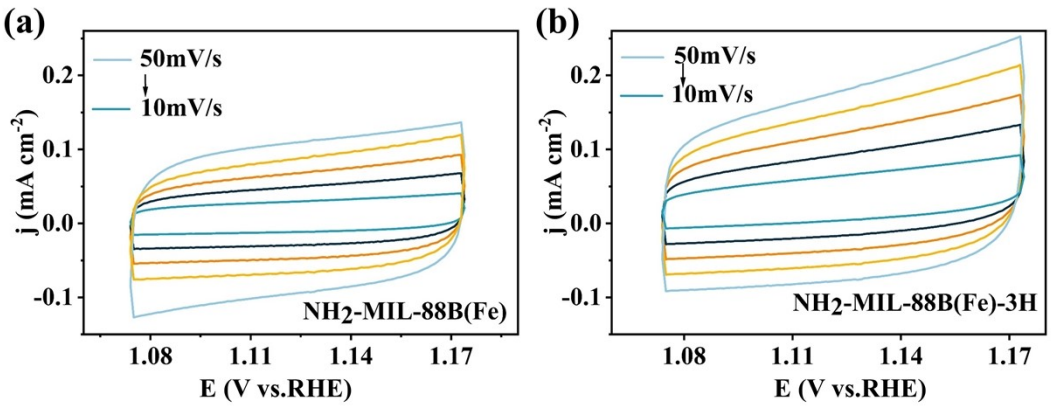

Figure. S11 CVs collected at various scan rates (10, 20, 30, 40 and 50 mV/s) for (a) NH_2-MIL-88B(Fe)-3H, (b) NH_2-MIL-88B(Fe) in 1 M KOH.

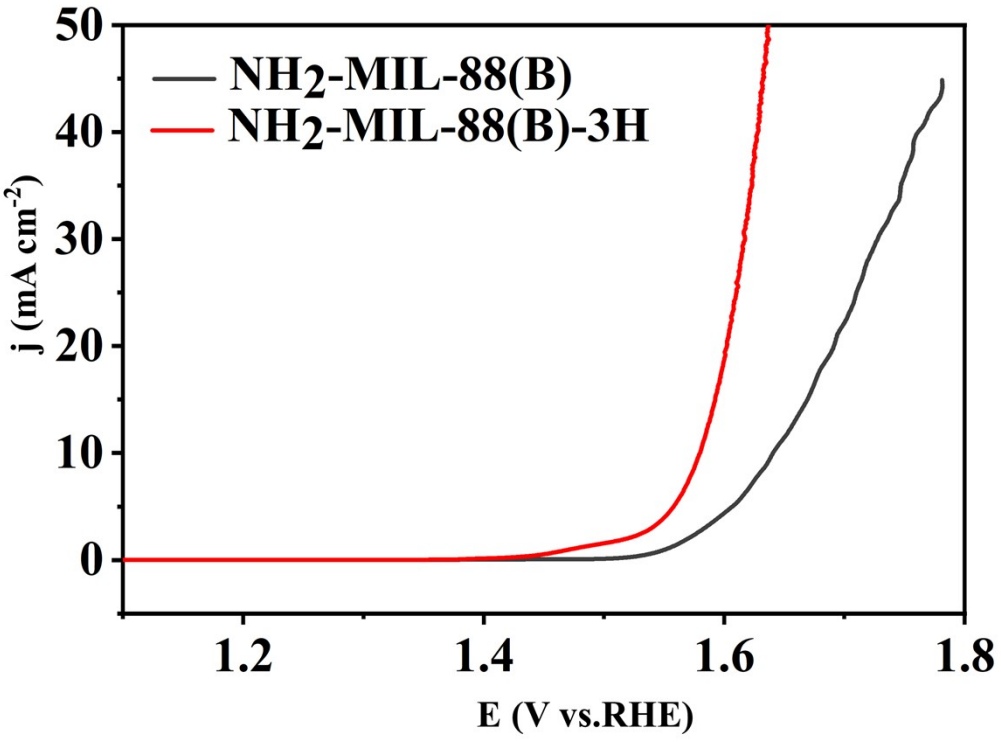

Figure. S12 Polarization curves of catalysts based on ECSA.

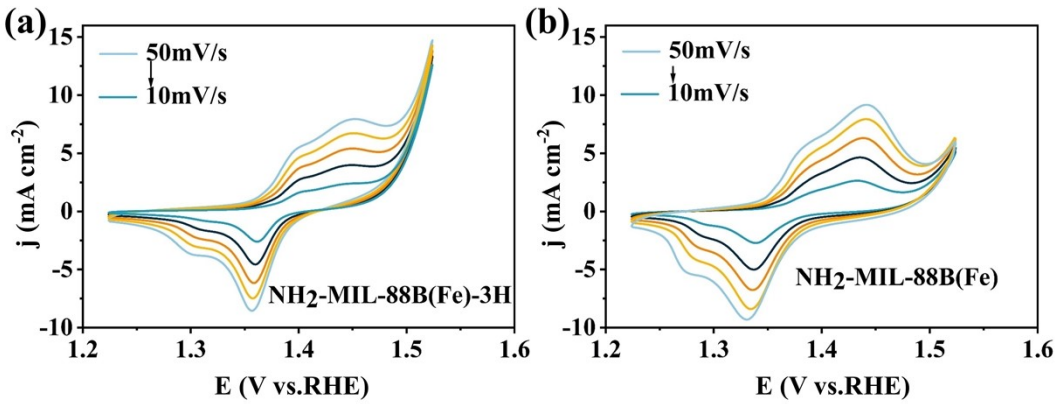

Figure. S13 CVs with different scan rates (10, 20, 30, 40 and 50 mV/s) in 1 M KOH of (a) NH_2-MIL-88B(Fe)-3H; (b) NH_2-MIL-88B(Fe) in 1 M KOH.

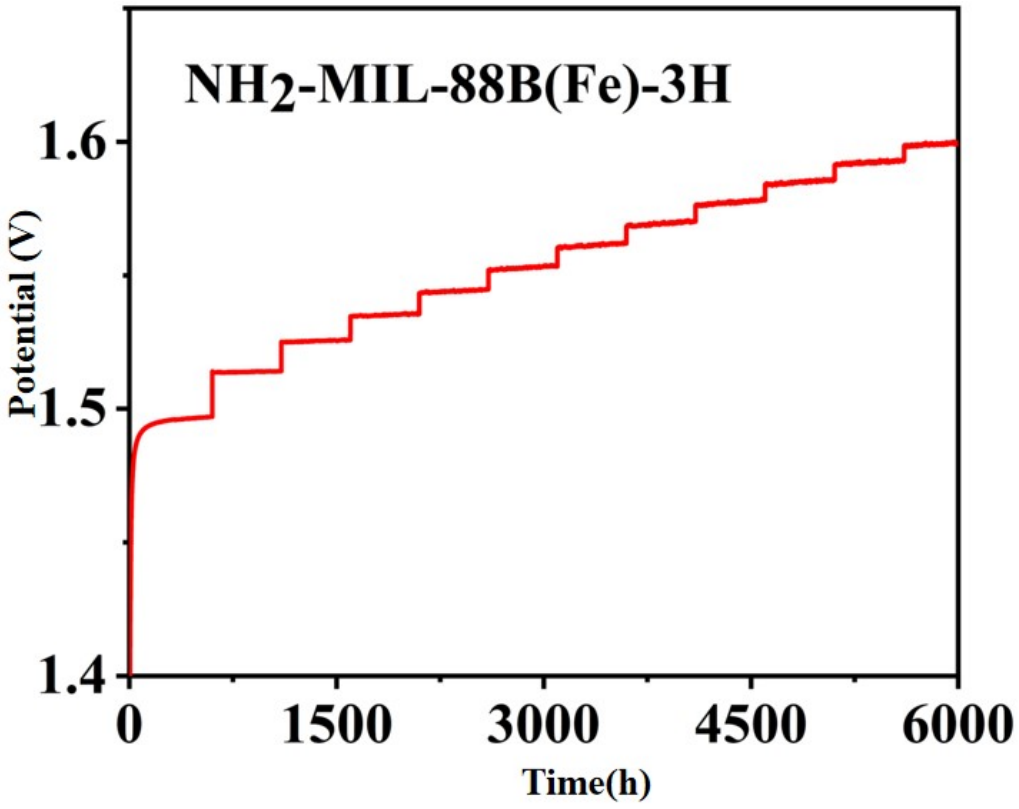

Figure. S14 The multi-current process curve of NH_2-MIL-88B(Fe)-3H without iR correction.

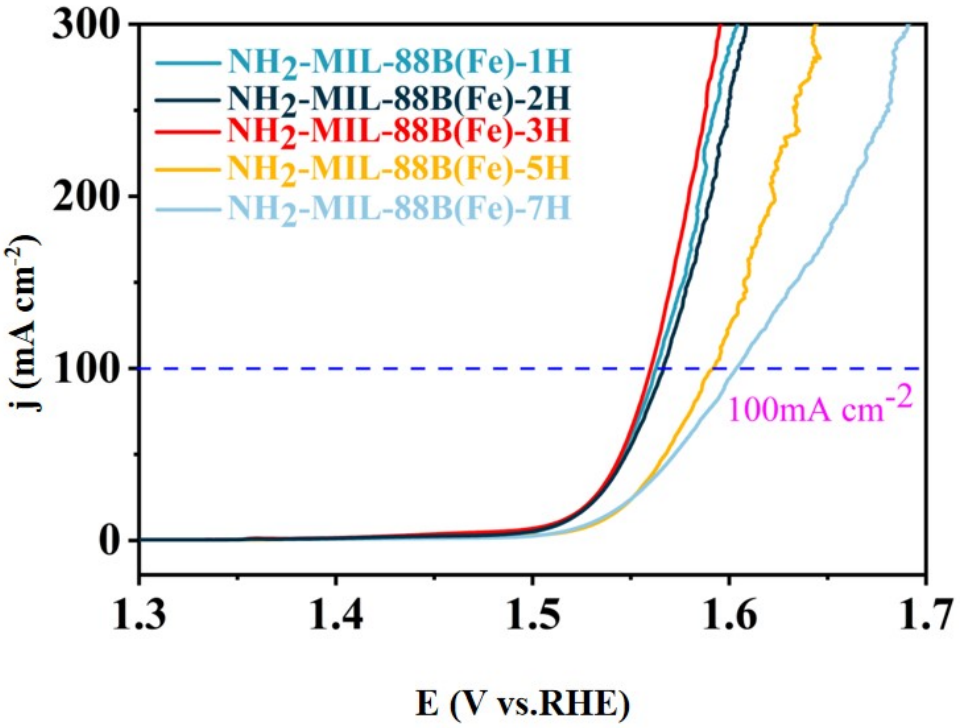

Figure. S15 Comparison of overpotential magnitudes at different current densities in 1 M KOH + 0.5 M NaCl.

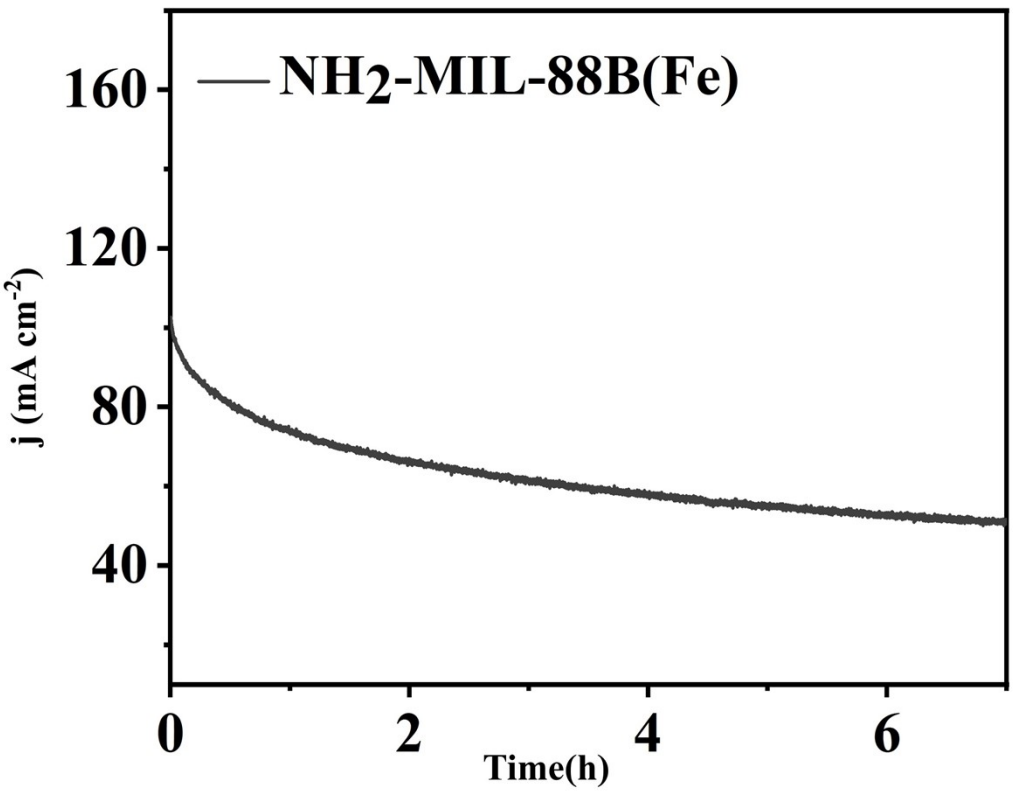

Figure. S16 Long-term stability test in 1 M KOH + 0.5 M NaCl over 7 h of NH_2-MIL-88B(Fe)

Table S1. Comparison of catalytic performance for NH_2-MIL-88B(Fe)-3H with other reported OER at 100 mA cm^{-2}.

Catalyst	j (mA cm^{-2})	η (mV)	Electrolyte	Ref.
NH_2-MIL-88B(Fe)-3H	100	313	1.0 M KOH	This work
NH_2-MIL-88B(Fe)	100	367	1.0 M KOH	This work
Co-NiFeLDH	100	335	1.0 M KOH	[3]
NCP-5	100	410	1.0 M KOH	[4]
NiCo-300	100	390	1.0 M KOH	[5]
MnCoP/NF	100	415	1.0 M KOH	[6]
Mo-NiOOH	100	390	1.0 M KOH	[7]
F-NiFeLDH	100	349	1.0 M KOH	[8]
W- FeCoLDH	100	330	1.0 M KOH	[9]
np-NiMnFeMo	100	324	1.0 M KOH	[10]
Co_1Mn_1CH	100	349	1.0 M KOH	[11]
$Ni(OH)_2$/F-Ni_3S_2	100	360	1.0 M KOH	[12]

References

[1] Y. Huang, L.W. Jiang, B.Y. Shi, K.M. Ryan, J.J. Wang, Highly Efficient Oxygen Evolution Reaction Enabled by Phosphorus Doping of the Fe Electronic Structure in Iron–Nickel Selenide Nanosheets, Advanced Science, 8 (2021) e2101775.

[2] P.F. Guo, Y. Yang, B. Zhu, Q.N. Yang, Y. Jia, W.T. Wang, Z.T. Liu, S.Q. Zhao, X. Cui, Heterostructural NiFeW disulfide and hydroxide dual-trimetallic core-shell nanosheets for synergistically effective water oxidation, Carbon Energy, (2024) e532.

[3] Y. Yang, S. Wei, Y. Li, D. Guo, H. Liu, L. Liu, Effect of cobalt doping-regulated crystallinity in nickel-iron layered double hydroxide catalyzing oxygen evolution, Applied Catalysis B: Environmental, 314 (2022) 121491.

[4] D.-H. Park, M.-H. Kim, M. Kim, J.-H. Byeon, J.-S. Jang, J.-H. Kim, D.-M. Lim, S.-H. Park, Y.-H. Gu, J. Kim, K.-W. Park, Spherical nickel doped cobalt phosphide as an anode catalyst for oxygen evolution reaction in alkaline media: From catalysis to system, Applied Catalysis B: Environmental, 327 (2023) 122444.

[5] B. Zhang, X. Zhang, Y. Wei, L. Xia, C. Pi, H. Song, Y. Zheng, B. Gao, J. Fu, P.K. Chu, General synthesis of NiCo alloy nanochain arrays with thin oxide coating: a highly efficient bifunctional electrocatalyst for overall water splitting, Journal of Alloys and Compounds, 797 (2019) 1216-1223.

[6] W.-Y. Fu, Y.-X. Lin, M.-S. Wang, S. Si, L. Wei, X.-S. Zhao, Y.-S. Wei, Sepaktakraw-like catalyst Mn-doped CoP enabling ultrastable electrocatalytic oxygen evolution at 100 mA·cm−2 in alkali media, Rare Metals, 41 (2022) 3069-3077.

[7] Y. Jin, S. Huang, X. Yue, C. Shu, P.K. Shen, Highly stable and efficient non-precious metal electrocatalysts of Mo-doped NiOOH nanosheets for oxygen evolution reaction, International Journal of Hydrogen Energy, 43 (2018) 12140-12145.

[8] M. Li, Y. Gu, Y. Chang, X. Gu, J. Tian, X. Wu, L. Feng, Iron doped cobalt fluoride derived from CoFe layered double hydroxide for efficient oxygen evolution reaction, Chemical Engineering Journal, 425 (2021) 130686.

[9] X. Liang, F.-K. Chiang, L. Zheng, H. Xiao, T. Zhang, F. Zhang, Q. Gao, High-content atomically distributed W(v,vi) on FeCo layered double hydroxide with high oxygen evolution reaction activity, Chemical Communications, 58 (2022) 7678-7681.

[10] H. Liu, C. Xi, J. Xin, G. Zhang, S. Zhang, Z. Zhang, Q. Huang, J. Li, H. Liu, J. Kang, Free-standing nanoporous NiMnFeMo alloy: An efficient non-precious metal electrocatalyst for water splitting, Chemical Engineering Journal, 404 (2021) 126530.
[11] T. Tang, W.-J. Jiang, S. Niu, N. Liu, H. Luo, Y.-Y. Chen, S.-F. Jin, F. Gao, L.-J. Wan, J.-S. Hu, Electronic and Morphological Dual Modulation of Cobalt Carbonate Hydroxides by Mn Doping toward Highly Efficient and Stable Bifunctional Electrocatalysts for Overall Water Splitting, Journal of the American Chemical Society, 139 (2017) 8320-8328.
[12] P. Hao, W. Zhu, F. Lei, X. Ma, J. Xie, H. Tan, L. Li, H. Liu, B. Tang, Morphology and electronic structure modulation induced by fluorine doping in nickel-based heterostructures for robust bifunctional electrocatalysis, Nanoscale, 10 (2018) 20384-20392.